Amyloid-β-induced astrocytic phagocytosis is mediated by CD36, CD47 and RAGE

Raasay S. Jones, Aedín M. Minogue[§], Thomas J. Connor and Marina A. Lynch.

Trinity College Institute of Neuroscience,

Department of Physiology,

Lloyd Building,

Trinity College,

Dublin 2.

Ireland.

[§]Corresponding author:

E-mail: aminogu@tcd.ie

Phone: +353 1 8968476

Fax: +353 1 8963183

ABSTRACT

Astrocytes, the most numerous glial cell in the brain, have multiple functions and are key to maintenance of homeostasis in the central nervous system. Microglia are the resident immunocompetent cells in the brain and share several functions with macrophages, including their phagocytic ability. Indeed microglia are the resident phagocytes in the brain and express numerous cell surface proteins which act to enable receptor-mediated phagocytosis. However recent evidence suggests that astrocytes express some genes which permit phagocytosis of phosphatidylserine-decorated cells and this probably explains sporadic reports in the literature which suggest that astrocytes become phagocytic following brain trauma. Here we examined the potential of astrocytes to phagocytose fluorescently-labelled latex beads and amyloid-β (Aβ) and report that they competently engulf both in a manner that relies on actin polymerization since it was inhibited by cytochalasin D. The data indicate that incubation of cultured astrocytes or microglia with Aβ increased phagocytosis and markers of activation of both cell types. Aβ was found to markedly increase expression of the putative Aβ-binding receptors CD36 and CD47 in astrocytes, while it decreased expression of the receptor for advanced glycation endproducts (RAGE). It is demonstrated that blocking these receptors using a neutralizing antibody attenuated Aβ-induced phagocytosis of latex beads by astrocytes. Interestingly blocking these receptors also decreased uptake of beads even in the absence of Aβ. Here we demonstrate that astrocytes are competent phagocytes and are capable of engulfing Aβ.

Key words: astrocyte, phagocytosis, FITC-tagged amyloid-β, CD36, CD47 and RAGE.

INTRODUCTION

Phagocytosis is an essential element of the innate immune response, an important defence mechanism against infection and the process by which cell debris is removed. In the CNS,

microglia are the resident immunocompetent cells, sharing several characteristics with peripheral macrophages including their phagocytic function.

Evidence from numerous sources indicates that microglia mediate the clearance of Aβ though receptor-mediated phagocytosis, and potential roles for several receptors have been described; these include the receptor for advanced glycation end products (RAGE), Toll-like receptors 2 and 4, the scavenger receptor CD36, phosphatidylserine (PS) receptor and the purine receptor P_2Y_6 (Noda and Suzumura 2012). Uptake of Aβ by microglia, and its subsequent targeting to the endosome-lysosomal pathway, has been examined in detail with microglia shown to actively phagocytose monomeric, oligomeric and fibrillar Aβ (Lee and Landreth 2010) while ultrastructural studies have identified intra-cytoplasmic fragments of Aβ in microglia in models of AD (Mandrekar-Colucci et al. 2012) and in post-mortem tissue prepared from AD patients (Lewandowska et al. 2004). However, there is inefficient clearance of amyloid-β (Aβ) in the brain in Alzheimer's disease (AD) and a great deal of evidence suggests that accumulation of Aβ in the brain contributes to pathogenesis of the disease. It has been shown that phagocytosis of Aβ by macrophages prepared from patients with AD is decreased (Mizwicki et al. 2012), but the phagocytic capacity of microglia in AD patients is not known. However a recent study reported that CD68 expression was increased in post-mortem brain tissue obtained from AD patients which had been immunized with Aβ (AN1792); this correlated with Aβ load and, although implied rather than explicit, this perhaps suggests that the phagocytic potential of microglia was reduced in AD patients (Zotova et al. 2011).

It has been suggested that early microglial activation, and specifically recruitment of bone marrow-derived cells, may limit Aβ accumulation (Simard et al. 2006; El Khoury et al. 2007), whereas persistent activation appears to parallel the increase in plaque development. This is consistent with the finding that, with age, microglia become dystrophic and functionally deficient (Streit et al. 2009), and with the observation that microglial expression of several Aβ-binding proteins, which play a role in phagocytosis, decreases with age in APPswe/PS1dE9 mice (Hickman et al. 2008).

In comparison to microglia, the role of astrocytes as phagocytic cells is less studied. It is recognized that astrocytes do not express certain genes associated with phagocytosis in microglia, although a recent study suggests that the molecular machinery required for phagocytosis of phosphatidylserine-labelled apoptotic cells is present in astrocytes. Expression of certain genes of the cell death abnormality (ced) pathway are expressed on astrocytes (Cahoy et al. 2008) including ced-1 and ced-7, which regulate expression of phosphatidylserine on phagocytic cells (Mapes et al. 2012) and the integrin αvβ5, which modulates stabilin-2-mediated phagocytosis (Kim et al. 2012). This provides a mechanism by which astrocytes engulf and break down myelin (Lantos 1974), play a role in axon elimination (Berbel and Innocenti 1988) and phagocytose large axonal evulsions (Nguyen et al. 2011). Astrocytes have also been shown to become phagocytic following brain trauma (al-Ali and al-Hussain 1996; Bechmann and Nitsch 1997).

There have been few studies designed to examine a role for astrocytes in clearance of Aβ although a decrease in Aβ levels was reported when astrocytes were applied to brain sections prepared from a mouse model of AD (Wyss-Coray et al. 2003). In addition, astrocytes from enhanced green fluorescent protein-expressing mice transplanted into the hippocampus of APPswe/PS1dE9 mice were found to internalise Aβ immunoreactive material (Pihlaja et al. 2008).

In this study, we set out to examine the phagocytic potential of astrocytes *in vitro* and report that these cells efficiently phagocytose fluorescently-labelled latex beads and fluorescently-labelled (FITC-tagged) Aβ. Incubation of cells in the presence of Aβ increased markers of glial activation and stimulated phagocytosis in astrocytes as well as microglia. The data indicate that incubation of cultured astrocytes with Aβ markedly increased expression of the putative Aβ binding receptors CD36 and CD47 in astrocytes, while it decreased expression of RAGE. It is demonstrated that blocking these proteins using a neutralizing antibody attenuated Aβ-induced phagocytosis of latex beads by astrocytes, in addition to decreasing uptake of beads even in the absence of Aβ.

METHODS

Preparation of cultured cells

Primary mixed glial cell cultures were prepared from brains of 1-3 day old neonatal Wistar rats (Bioresources Unit, Trinity College, Dublin, Ireland). The meninges and adherent blood vessels were removed, cortical tissue was dissected, cross-chopped and incubated (20 min, 37°C) in Dulbecco's modified Eagle's medium (DMEM; Invitrogen, UK) supplemented with 10% fetal bovine serum and 50 U/ml penicillin/streptomycin (Invitrogen, UK). Tissue was triturated, passed though a nylon cell strainer (40μM) and centrifuged (2000rpm, 3 min, 20°C). Cells were counted, plated onto 6-well plates (density: $1x10^6$ cells/ml) and maintained at 37°C in a 5% CO_2 humidified atmosphere. Culture media was replaced every 3-4 days until cells reached confluency.

After 10 days, mixed glia were pretreated with cytochalasin D (1-10μM; Calbiochem, Germany) or vehicle control for 2 h prior to examining phagocytosis or 4 h prior to assessing cell viability using alamar blue and LDH assays.

Purified astrocytes or microglia were used for analysis of zymosan phagocytosis, and for the experiments in which we assessed the effect of neutralising antibodies. To prepare purified microglial cultures, cells were seeded onto T25 flasks and, after 24 h, media was replaced with DMEM containing M-CSF (20ng/ml; R&D Systems, UK) and GM-CSF (10ng/ml; R&D Systems, UK). After 10 days, flasks were shaken (2 h, 130rpm, room temperature) and tapped several times to remove nonadherent microglia. Supernatants were centrifuged (2000rpm, 3 min, 20°C) and the resultant pellet was resuspended in DMEM. Cells were counted, plated onto 6-well plates (density: $1x10^6$ cells/ml) and maintained at 37°C in a 5% CO_2 humidified atmosphere for 2 days prior to treatment.

Purified astrocytes were prepared as described for mixed glia except that, on day 10, microglia were removed by shaking (2 h, 200rpm, room temperature). The supernatant was removed, adherent astrocytes were washed with phosphate-buffered saline (PBS) and incubated with 0.05% w/v trypsin-ethylene diamine tetraacetic acid (EDTA) at 37°C until cells began to detach. DMEM was added to terminate the action of trypsin, cells were centrifuged (2000rpm, 3

min, 20°C), plated onto 6-well plates (density: 1×10^6 cells/ml) and maintained at 37°C in a 5% CO_2 humidified atmosphere for 2 days prior to treatment.

Lyophilized $A\beta_{1-40}$, $A\beta_{1-42}$ and $A\beta_{40-1}$ peptides (Invitrogen, UK) were dissolved in HPLC grade water to provide a 6mg/ml stock solution, diluted to 1mg/ml using sterile PBS and allowed to aggregate (48 h, 220 rpm, 37°C). Isolated cultures of microglia and astrocytes were incubated with $A\beta_{1-40}$ (4.2μM) + $A\beta_{1-42}$ (5.8μM), or $A\beta_{40-1}$ (10μM) for 24 h at 37°C.

In a further set of experiments, astrocytes were incubated with $A\beta$ cocktail or reverse peptide in the presence of anti-CD36 rabbit polyclonal, anti-CD47 mouse monoclonal (Santa Cruz Biotechnology, USA) or anti-RAGE goat polyclonal (R&D Systems, UK) neutralizing antibodies or rabbit, mouse or goat IgG controls (Santa Cruz Biotechnology, USA; R&D Systems, UK; all at 2.5μg/ml) respectively for 24 h prior to assessing phagocytosis.

Analysis of cell viability

Lactate dehydrogenase (LDH) and alamar blue assays were used to evaluate cell viability. The LDH CytoTox 96® assay (Promega, UK) was carried out as per manufacturer's instructions. Aliquots of supernatants (50μl) were transferred to a 96-well flat-bottomed plate. DMEM alone was used as the negative control and supernatant from cells incubated in the presence of lysis buffer as the positive control. Reconstituted substrate mix (50μl) was added to each well and the plate was incubated in the dark at room temperature for 30 min. Stop solution (50μl) was added and the absorbance was read at 490nm. Cytotoxicity (%) was calculated as the (absorbance in samples/maximum absorbance) x 100.

The alamar blue assay is based upon the ability of viable cells to reduce resazurin to resorufin with the amount of fluorescence produced being proportional to the number of living cells. A stock solution of resazurin (440μM in dH_2O; Sigma, UK) was added to cells at a 1:10 dilution in DMEM, with the appropriate controls as described above. Cells were incubated at at 37°C until a colour change was observed (pink in viable cells and dark blue in non-viable cells), at which time absorbance in aliquots of supernatant (100μl) was read at 595nm. Cell viability was assessed as follows: % Cell viability = ((Am - As)/(Am - Ac)) x 100, where Am was the

absorbance in samples containing DMEM only, As was the average absorbance of wells containing cells without treatments and Ac was the absorbance of a particular sample.

Opsonized zymosan assay

To opsonize zymosan, serum was obtained from whole rat blood by centrifugation (4000rpm, 15 min, 4°C). Zymosan (1mg/ml; Sigma, UK) was diluted in Hank's balanced salt solution (HBSS; Sigma, UK) and incubated with serum (ratio 3:1, zymosan: serum; 30 min, 37°C). Samples were centrifuged (1600rpm, 10 min), the opsonized zymosan pellet was washed, centrifuged and resuspended in HBSS. Opsonized zymosan (50μl) was added to each well of a black 96-well microplate containing purified microglia, astrocytes or PBMCs, prepared from rat blood by density separation over Lymphoprep™ (50μl; $3x10^6$ cells/ml in HBSS) and luminol solution (1mM; 50μl) was added. Chemiluminescence measurements were taken at 2 minute intervals for 44 min.

Microscopy

Cells were fixed in ice-cold methanol (5 min, -20°C), washed 3 times (PBS containing 0.02% Triton X-100), blocked in 10% normal goat serum (2 h, room temperature) and incubated with mouse anti-rat CD11b (1:200; Serotec, US) or rabbit anti-GFAP (1:2000; Dako, Denmark) antibodies in 5% goat serum in wash buffer (overnight, 4°C). Coverslips were washed, incubated in the dark for 2 h with Alexa Fluor® 633 goat anti-mouse or goat anti-rabbit antibodies (1:4000 in 5% goat serum in wash buffer; Invitrogen, UK). Cells were washed, mounted onto glass slides using Vectashield with DAPI (Vector Labs, UK), sealed and stored at 4°C for fluorescent microscopy. Images were acquired using a LSM 510 Confocal Laser Scanning Microscope and visualized using LSM Image Browser Rel. 4.2. Z-stacking was carried out to obtain images of planes of the cell at various depths in order to confirm that fluorescently-labelled latex beads or FITC-Aβ had been internalized by cells of interest. Lysosomes were visualised by incubating astrocytes with Lysotracker® Red DND-99 (50nM in DMEM; Invitrogen, UK) for 2 h at 37°C prior to staining for GFAP.

FACS analysis

To assess phagocytosis, mixed glial cells, microglia or astrocytes were incubated with fluorescently-labelled yellow/green latex beads (Abs/Em=470/505nm; 1:200 dilution; 1μM; Sigma, UK) or HiLyte Fluor™ 488-labeled Aβ (Abs/Em=503/528nm; 0.15-10μM; Anaspec, US) for 2 h. Media was replaced with trypan blue (0.2mg/ml; Sigma, UK) and samples were incubated for 2 min to quench extracellular fluorescence. Cells were washed with FACS buffer (2% FBS, 0.1% NaN$_3$ in PBS), centrifuged (1200rpm, 5 min), resuspended in blocking solution (50% FBS in FACS buffer) for 30 min, centrifuged (1200rpm, 5 min) and resuspended in FACS buffer with Alexa Fluor 647 anti-rat CD11b (1:100; Serotec, UK) or APC anti-GLAST ACSA-1 (1:200; Miltenyi Biotec, US) for 30 min in order to identify CD11b$^+$ microglia and CD11b$^-$ or GLAST$^+$ astrocytes.

Unstained cells and fluorescence minus one (FMO) tubes were used to gate the percentage of positive cells in any channel. Compensation beads were used to optimise fluorescence settings for multicolour flow cytometric analyses. Phagocytic cells were represented as the number of CD11b$^+$ or CD11b$^-$ or GLAST$^+$ cells respectively positive in the fluorescein isothiocyanate (FITC) channel.

Assessment of mRNA expression of CD11b, GLT-1 and GFAP

RNA was extracted from harvested cultured cells using a NucleoSpin RNA II isolation kit (Macherey-Nagel Inc., Germany) and concentrations were equalized to 1μg prior to cDNA synthesis using a High Capacity cDNA RT Kit (Applied Biosystems, UK), according to the manufacturer's instructions. Equal concentrations of cDNA were used for RT-PCR amplification. Real-time PCR primers were delivered as "Taqman$^®$ Gene Expression Assays" containing forward and reverse primers, and a FAM-labeled MGB Taqman probe for each gene (Applied Biosystems, UK) as described previously (Downer et al. 2010). The assay IDs were as follows: CD11b (Rn00709342_m1), GLAST (Rn00570130_m1), GLT-1 (Rn00568080_m1), CD36 (Rn01442639_m1), CD47 (Rn00569914_m1) and RAGE (Rn00584249_m1). Gene

expression was calculated relative to the endogenous control samples (β-actin) to give a relative quantification (RQ) value (2^{-DDCT}, where CT is threshold cycle).

Statistical analysis

Data were analyzed using either Student's *t*-test for independent means or a one-way analysis of variance (ANOVA) followed by post hoc Student Newman–Keuls test to determine which conditions were significantly different from each other. Data are expressed as means with standard errors and deemed statistically significant when $p < 0.05$.

RESULTS

Mixed glia were incubated in the presence of fluorescently-labelled latex beads and stained with anti-GFAP. The data indicate the presence of fluorescently-labelled beads in both GFAP$^+$ and GFAP$^-$ cells (Figure 1A). Z-stack images, taken at planes of various depth within the cells, indicate that beads were internalized in both CD11b$^+$ cells (Figure 1B) and GFAP$^+$ cells (Figure 1C). We also confirm the presence of lysosomes, using lysotracker, in GFAP$^+$ cells (Figure 1D). These data indicate that, in addition to microglia, astrocytes are phagocytic and, consistent with this, we confirm that pretreatment of cells with cytochalasin D significantly inhibited uptake of latex beads in CD11b$^+$ and CD11b$^-$ cells (***$p < 0.001$; ANOVA; Figure 2A,B); cytochalasin D did not affect cell viability, as assessed by alamar blue (Figure 2C) or LDH release (Figure 2D) although, as predicted, staurosporine (5μm) significantly decreased cell viability (***$p < 0.001$; ANOVA) and increased LDH activity (***$p < 0.001$; ANOVA).

In addition to their ability to phagocytose latex beads, GFAP$^+$ cells also phagocytose Aβ. Analysis of the uptake of FITC-labelled Aβ revealed a concentration-dependent change in both uptake by CD11b$^+$ and CD11b$^-$ cells as revealed by the mean values (**$p < 0.01$; ***$p < 0.001$; ANOVA; Figure 3A, B) and the representative FACS-plots which illustrate the increase in the number of FITC$^+$ cells as the FITC-labelled Aβ concentration increased from zero to 10μM (Figure 3C). Pre-treatment with cytochalasin D partially but significantly decreased uptake of FITC-labelled Aβ by both CD11b$^+$ and CD11b$^-$ cells (**$p < 0.01$; ***$p < 0.001$; ANOVA; Figure

3D,E) and the inhibitory effect was significantly greater when cells were incubated in the presence of 10μM cytochalasin D compared with 1 and 3μM cytochalasin D ([+]p<0.05; ANOVA). Since the effect of cytochalasin D was partial, it was important to establish that FITC-Aβ was internalized by these cells and thus Z-stack confocal microscopy was employed to confirm the presence of Aβ within CD11b^{+} microglia and GFAP^{+} astrocytes respectively (Figure 4A,B). We also compared the oxidative burst in response to opsonized-zymosan in purified astrocytes and microglia to that of PBMCs and demonstrate that, although a significant phagocytic response was observed in both types of glia (p<0.01; ANOVA; Figure 5), it was markedly less than the response of PBMCs (p<0.001; ANOVA).

Having shown the phagocytic potential of astrocytes we investigated the effect of Aβ on phagocytic function in purified microglia and astrocytes *in vitro*. When purified microglia were incubated in the presence of Aβ, expression of CD11b mRNA was significantly increased (***p<0.001; Student's *t*-test for independent means; Figure 6A). Significant increases in CD40 mRNA and CD68 mRNA expression (1.00 ± 0.03 (control) vs 1.69 ± 0.11 (Aβ) and 1.01 ± 0.06 (control) vs 1.79 ± 0.13 (Aβ) respectively; p<0.001; Student's *t*-test for independent means) were also observed (data not shown). Aβ also significantly increased the percentage of CD11b^{+} bead^{+} cells (*p <0.05; Student's *t*-test for independent means; Figure 6B, C). Incubation of purified astrocytes in the presence of Aβ increased GLT-1 mRNA (***p <0.001; Student's *t*-test for independent means; Figure 6E) but had no effect on GLAST mRNA expression (Figure 6D). However, Aβ significantly increased the percentage of GLAST[+] bead^{+} cells (***p <0.001; Student's *t*-test for independent means; Figure 6F, G). Therefore the evidence indicates that Aβ stimulates purified microglia and astrocytes to phagocytose fluorescently-labelled latex beads.

Several cell surface proteins have been proposed to play a role in phagocytosis; these include RAGE, a class B scavenger receptor, CD36, and the membrane glycoprotein CD47 (Matozaki et al. 2009; Greenberg et al. 2006; Friggeri et al. 2011). These proteins have also been identified as Aβ-binding proteins (Koenigsknecht and Landreth 2004; Wilkinson and El Khoury 2012). Here, we first assessed the effect of Aβ on expression of these markers on astrocytes and show that it significantly increased CD36 and CD47 mRNA (Figure 7A,C) but decreased RAGE

mRNA expression (Figure 7E). Neutralising antibodies were assessed for their affinity for the target protein by western blot (data not shown). Whereas Aβ increased the proportion of latex bead[+] astrocytes (*p < 0.05; Figure 7B,D,F) as shown earlier, incubation of cells in the presence of anti-CD36, anti-CD47 or anti-RAGE antibodies decreased phagocytosis even in the absence of Aβ ([+]p < 0.05; [++]p < 0.01; ANOVA; control in the presence of IgG vs anti-CD36 or anti-CD47 or anti-RAGE) and significantly attenuated the Aβ-induced change ([+]p < 0.05; [++]p < 0.01; ANOVA; Aβ in the presence of IgG vs Aβ in the presence of anti-CD36 or anti-CD47 or anti-RAGE; Figure 7B,D,F; ANOVA).

DISCUSSION

We set out to assess the phagocytic potential of astrocytes and report that these cells actively phagocytose fluorescently-labelled latex beads, and FITC-labelled Aβ and that phagocytosis of opsonized zymosan by these cells is associated with a respiratory burst. The data indicate that Aβ stimulates uptake of fluorescently-labelled latex beads into astrocytes and that this is attenuated by blocking CD47, CD36 or RAGE.

Fluorescently-labelled latex beads and FITC-labelled Aβ were taken up in a concentration-dependent manner by both microglia and astrocytes. It is suggested that this occurred by phagocytosis since uptake was inhibited by cytochalasin D which blocks the actin polymerization on which phagocytosis relies. The phagocytic function of activated microglia has been known for decades. In contrast there are relatively few reports in the literature which indicate that astrocytes have phagocytic potential; astroglial filaments were found adjacent to demyelinating myelin sheaths in experimental gliomas, which they were shown to phagocytose and process (Lantos 1974), while astrocytes, as well as microglia, play a phagocytic role in axon elimination during embryonic and early post-natal development (Berbel and Innocenti 1988). More recently, a population of constitutively-phagocytic astrocytes, capable of engulfing large axonal evulsions, were identified in the postlaminar optic nerve head myelination transition zone; these astrocytes expressed Mac-2, a protein typically expressed on phagocytic cells (Nguyen et al. 2011). Astrocytes have also been shown to become phagocytic following brain

trauma; in particular, they are able to engulf colloidal carbon particles following their injection into the brain (al-Ali and al-Hussain 1996) while phagocytic astrocytes appear in the middle molecular layer of the dentate gyrus 6 days after lesioning of the entorhinal cortex (Bechmann and Nitsch 1997) and engulf TUNEL^{+} cells following traumatic brain injury *in vivo* (Loov et al. 2012). Although astrocytes do not express certain genes associated with phagocytosis in microglia, expression of specific genes of the cell death abnormality (ced) pathway are expressed on astrocytes (Cahoy et al. 2008) including ced-1 and ced-7, which regulate expression of phosphatidylserine on phagocytic cells (Mapes et al. 2012) and the integrin αvβ5, which modulates stabilin-2-mediated phagocytosis (Kim et al. 2012). Therefore the finding that astrocytes, as well as microglia, had the ability to internalise soluble Cy3-labeled Aβ *in vitro* is not unexpected (Mandrekar et al. 2009). However, this group reported that the phagocytic ability of astrocytes was much less efficient and more variable than microglia, with one population of cells capable of internalizing Aβ as efficiently as microglia while other populations exhibited no phagocytic capability. In the present study the efficiency of astrocytes to phagocytose latex beads and FITC-labelled Aβ was similar to that of microglia and therefore the marked cell-associated difference in phagocytic ability in terms of soluble Aβ was not evident when phagocytosis of aggregated Aβ was examined.

Cytochalasin D did not completely abrogate the uptake of beads or Aβ and this indicates that both may be partially internalized by a mechanism independent of actin-polymerisation, as has been described in the case of polystyrene particles which were taken up by phagocytic cells even in the presence of cytochalasin D (Hofer et al. 2009). The possibility that Aβ simply adhered to the cell membrane and was not internalized does not provide an explanation for the findings since extracellular fluorescence was routinely quenched using trypan blue which discriminates between adherent and ingested fluorescent particles (Van Amersfoort and Van Strijp 1994), and Z-stack confocal microscopy indicated the intracellular localization of Aβ. Uptake of FITC-labelled Aβ was concentration-dependent, which was not the case with latex beads; this raises the possibility that different uptake methods exist for latex beads and Aβ.

Zymosan-induced luminol-enhanced chemiluminescence was also used to compare the phagocytic responses of microglia and astrocytes and the evidence indicated that the production of reactive oxygen species occurred in both cell types; the response of microglia was somewhat greater than astrocytes, while both were markedly less than the response of PBMCs.

There are conflicting data regarding the modulatory effect of inflammatory cytokines on phagocytosis by microglia, with some groups suggesting a stimulatory effect on phagocytosis (Shaftel et al. 2007; Chakrabarty et al. 2010) and others reporting the opposite (Koenigsknecht-Talboo and Landreth 2005). Aβ stimulates production and release of several inflammatory cytokines from microglia and astrocytes (Floden and Combs 2006; Lindberg et al. 2005; Benveniste et al. 2001; Butovsky et al. 2005; Veerhuis et al. 2005), but here we investigated the effect of Aβ on phagocytosis. Aβ increased mRNA expression of CD11b and the uptake of latex beads by CD11b$^+$ microglia and it also increased expression of CD68. CD68 is a lysosome-associated membrane protein thought to be involved in a number of cellular processes including phagocytosis and autophagy (Zotova et al. 2011) . Given its role in these processes it seems likely that the upregulated expression of this protein seen here reflects an attempt to clear aggregated Aβ from the extracellular space. However, whether the upregulated expression of CD68 is preferentially associated with phagocytosis or autophagy remains to be elucidated - both processes are important in the clearance of misfolded or aggregated protein. Interestingly the ability of astrocytes to clear aggregated proteins in a number of neurodegenerative disease has been reported (Seidel et al. 2012). .

Having shown that Aβ triggers phagocytosis in astrocytes, we examined the possibility that this might rely on the association of Aβ with CD36, CD47 or RAGE. Aβ differentially affected the expression of CD36, CD47 and RAGE on astrocytes; while it markedly increased the expression of CD36 and CD47, it had the opposite effect on RAGE. The finding that these proteins are expressed on astrocytes is consistent with previous observations (Sick et al. 2011; Bao et al. 2012; Askarova et al. 2011) although earlier findings suggested that RAGE was expressed on microglia but not astrocytes (Alarcon et al. 2005).

We demonstrate that blocking each of these proteins using a neutralizing antibody attenuated Aβ-induced phagocytosis of latex beads by astrocytes. Interestingly the antibodies also decreased uptake of beads even in the absence of Aβ. A role for these proteins in phagocytosis by macrophages or microglia has been reported (Matozaki et al. 2009; Greenberg et al. 2006; Friggeri et al. 2011; Bao et al. 2012; Gitik et al. 2011) but, to our knowledge, there is no previous evidence that they play a role in phagocytosis by astrocytes. The fact that antibodies to these proteins attenuate Aβ-induced uptake of latex beads is not surprising since they all act as Aβ binding proteins (Koenigsknecht and Landreth 2004).

The phagocytic role of astrocytes may be more important than hitherto suspected, particularly in the context of the recent finding that ablation of microglia exerted no significant effect on Aβ accumulation in two transgenic mouse models of Alzheimer's disease, APP/PS1 and APP23 mice (Grathwohl et al. 2009). The findings indicated that the almost-complete absence of microglia for a 4 week period exerted no effect on either congophilic amyloid deposits or dystrophic neuritic structures indicating that the role of microglia, at least during a specific time period, exerts limited effect on *de novo* formation of amyloid-containing plaques and clearance of amyloid from plaques. It has been demonstrated, particularly in post-mortem human tissue that microglia become dystrophic with age and it is reasonable to assume that senescence adversely affects their function (Streit et al., 2009). The results obtained in this study may reflect impaired function associated with senescence of microglia. Although a similar senescence-associated change in the function of astrocytes remains to be demonstrated, expression of GFAP increases with age; whether this reflects enhanced phagocytic capacity or dysregulation of function remains to be elucidated (Lynch et al. 2010).

We conclude that astrocytes are competent phagocytes and their ability to engulf Aβ may be important in the context of identifying strategies which might reduce Aβ accumulation in Alzheimer's disease.

REFERENCES

al-Ali SY, al-Hussain SM (1996) An ultrastructural study of the phagocytic activity of astrocytes in adult rat brain. Journal of anatomy 188 (Pt 2):257-262

Alarcon R, Fuenzalida C, Santibanez M, von Bernhardi R (2005) Expression of scavenger receptors in glial cells. Comparing the adhesion of astrocytes and microglia from neonatal rats to surface-bound beta-amyloid. J Biol Chem 280 (34):30406-30415. doi:M414686200 [pii]

10.1074/jbc.M414686200

Askarova S, Yang X, Sheng W, Sun GY, Lee JC (2011) Role of Abeta-receptor for advanced glycation endproducts interaction in oxidative stress and cytosolic phospholipase A(2) activation in astrocytes and cerebral endothelial cells. Neuroscience 199:375-385. doi:S0306-4522(11)01092-X [pii]

10.1016/j.neuroscience.2011.09.038

Bao Y, Qin L, Kim E, Bhosle S, Guo H, Febbraio M, Haskew-Layton RE, Ratan R, Cho S (2012) CD36 is involved in astrocyte activation and astroglial scar formation. J Cereb Blood Flow Metab 32 (8):1567-1577. doi:jcbfm201252 [pii]

10.1038/jcbfm.2012.52

Bechmann I, Nitsch R (1997) Astrocytes and microglial cells incorporate degenerating fibers following entorhinal lesion: a light, confocal, and electron microscopical study using a phagocytosis-dependent labeling technique. Glia 20 (2):145-154

Benveniste EN, Nguyen VT, O'Keefe GM (2001) Immunological aspects of microglia: relevance to Alzheimer's disease. Neurochem Int 39 (5-6):381-391. doi:S0197018601000456 [pii]

Berbel P, Innocenti GM (1988) The development of the corpus callosum in cats: a light- and electron-microscopic study. The Journal of comparative neurology 276 (1):132-156. doi:10.1002/cne.902760109

Butovsky O, Talpalar AE, Ben-Yaakov K, Schwartz M (2005) Activation of microglia by aggregated beta-amyloid or lipopolysaccharide impairs MHC-II expression and renders them cytotoxic whereas IFN-gamma and IL-4 render them protective. Mol Cell Neurosci 29 (3):381-393. doi:S1044-7431(05)00056-4 [pii]

10.1016/j.mcn.2005.03.005

Cahoy JD, Emery B, Kaushal A, Foo LC, Zamanian JL, Christopherson KS, Xing Y, Lubischer JL, Krieg PA, Krupenko SA, Thompson WJ, Barres BA (2008) A transcriptome database for astrocytes, neurons, and oligodendrocytes: a new resource for understanding brain development and

function. The Journal of neuroscience : the official journal of the Society for Neuroscience 28 (1):264-278. doi:10.1523/JNEUROSCI.4178-07.2008

Chakrabarty P, Jansen-West K, Beccard A, Ceballos-Diaz C, Levites Y, Verbeeck C, Zubair AC, Dickson D, Golde TE, Das P (2010) Massive gliosis induced by interleukin-6 suppresses Abeta deposition in vivo: evidence against inflammation as a driving force for amyloid deposition. FASEB journal : official publication of the Federation of American Societies for Experimental Biology 24 (2):548-559. doi:10.1096/fj.09-141754

Downer EJ, Cowley TR, Lyons A, Mills KH, Berezin V, Bock E, Lynch MA (2010) A novel anti-inflammatory role of NCAM-derived mimetic peptide, FGL. Neurobiol Aging 31 (1):118-128. doi:S0197-4580(08)00101-2 [pii]

10.1016/j.neurobiolaging.2008.03.017

El Khoury J, Toft M, Hickman SE, Means TK, Terada K, Geula C, Luster AD (2007) Ccr2 deficiency impairs microglial accumulation and accelerates progression of Alzheimer-like disease. Nat Med 13 (4):432-438

Floden AM, Combs CK (2006) Beta-amyloid stimulates murine postnatal and adult microglia cultures in a unique manner. The Journal of neuroscience : the official journal of the Society for Neuroscience 26 (17):4644-4648. doi:26/17/4644 [pii]

10.1523/JNEUROSCI.4822-05.2006

Friggeri A, Banerjee S, Biswas S, de Freitas A, Liu G, Bierhaus A, Abraham E (2011) Participation of the receptor for advanced glycation end products in efferocytosis. J Immunol 186 (11):6191-6198. doi:jimmunol.1004134 [pii]

10.4049/jimmunol.1004134

Gitik M, Liraz-Zaltsman S, Oldenborg PA, Reichert F, Rotshenker S (2011) Myelin down-regulates myelin phagocytosis by microglia and macrophages through interactions between CD47 on myelin and SIRPalpha (signal regulatory protein-alpha) on phagocytes. J Neuroinflammation 8:24. doi:1742-2094-8-24 [pii]

10.1186/1742-2094-8-24

Grathwohl SA, Kalin RE, Bolmont T, Prokop S, Winkelmann G, Kaeser SA, Odenthal J, Radde R, Eldh T, Gandy S, Aguzzi A, Staufenbiel M, Mathews PM, Wolburg H, Heppner FL, Jucker M (2009) Formation and maintenance of Alzheimer's disease beta-amyloid plaques in the absence of microglia. Nature neuroscience 12 (11):1361-1363. doi:10.1038/nn.2432

Greenberg ME, Sun M, Zhang R, Febbraio M, Silverstein R, Hazen SL (2006) Oxidized phosphatidylserine-CD36 interactions play an essential role in macrophage-dependent phagocytosis of apoptotic cells. J Exp Med 203 (12):2613-2625. doi:jem.20060370 [pii]

10.1084/jem.20060370

Hickman SE, Allison EK, El Khoury J (2008) Microglial dysfunction and defective beta-amyloid clearance pathways in aging Alzheimer's disease mice. The Journal of neuroscience : the official journal of the Society for Neuroscience 28 (33):8354-8360. doi:10.1523/JNEUROSCI.0616-08.2008

Hofer U, Lehmann AD, Waelti E, Amacker M, Gehr P, Rothen-Rutishauser B (2009) Virosomes can enter cells by non-phagocytic mechanisms. J Liposome Res 19 (4):301-309. doi:10.3109/08982100902911612

Kim S, Park SY, Kim SY, Bae DJ, Pyo JH, Hong M, Kim IS (2012) Cross Talk between Engulfment Receptors Stabilin-2 and Integrin alphavbeta5 Orchestrates Engulfment of Phosphatidylserine-Exposed Erythrocytes. Molecular and cellular biology 32 (14):2698-2708. doi:10.1128/MCB.06743-11

Koenigsknecht-Talboo J, Landreth GE (2005) Microglial phagocytosis induced by fibrillar beta-amyloid and IgGs are differentially regulated by proinflammatory cytokines. The Journal of neuroscience : the official journal of the Society for Neuroscience 25 (36):8240-8249

Koenigsknecht J, Landreth G (2004) Microglial phagocytosis of fibrillar beta-amyloid through a beta1 integrin-dependent mechanism. The Journal of neuroscience : the official journal of the Society for Neuroscience 24 (44):9838-9846. doi:24/44/9838 [pii]

10.1523/JNEUROSCI.2557-04.2004

Lantos PL (1974) An electron microscope study of reacting astrocytes in gliomas induced by n-ethyl-n-nitrosourea in rats. Acta Neuropathol 30 (2):175-181

Lee CY, Landreth GE (2010) The role of microglia in amyloid clearance from the AD brain. J Neural Transm 117 (8):949-960. doi:10.1007/s00702-010-0433-4

Lewandowska E, Wierzba-Bobrowicz T, Kosno-Kruszewska E, Lechowicz W, Schmidt-Sidor B, Szpak GM, Bertrand E, Pasennik E, Gwiazda E (2004) Ultrastructural evaluation of activated forms of microglia in human brain in selected neurological diseases (SSPE, Wilson's disease and Alzheimer's disease). Folia Neuropathol 42 (2):81-91

Lindberg C, Selenica ML, Westlind-Danielsson A, Schultzberg M (2005) Beta-amyloid protein structure determines the nature of cytokine release from rat microglia. J Mol Neurosci 27 (1):1-12. doi:JMN:27:1:001 [pii]

10.1385/JMN:27:1:001

Loov C, Hillered L, Ebendal T, Erlandsson A (2012) Engulfing astrocytes protect neurons from contact-induced apoptosis following injury. PloS one 7 (3):e33090. doi:10.1371/journal.pone.0033090

Lynch AM, Murphy KJ, Deighan BF, O'Reilly JA, Gun'ko YK, Cowley TR, Gonzalez-Reyes RE, Lynch MA (2010) The impact of glial activation in the aging brain. Aging Dis 1 (3):262-278

Mandrekar-Colucci S, Karlo JC, Landreth GE (2012) Mechanisms Underlying the Rapid Peroxisome Proliferator-Activated Receptor-gamma-Mediated Amyloid Clearance and Reversal of Cognitive Deficits in a Murine Model of Alzheimer's Disease. The Journal of neuroscience : the official journal of the Society for Neuroscience 32 (30):10117-10128. doi:10.1523/JNEUROSCI.5268-11.2012

Mandrekar S, Jiang Q, Lee CY, Koenigsknecht-Talboo J, Holtzman DM, Landreth GE (2009) Microglia mediate the clearance of soluble Abeta through fluid phase macropinocytosis. The Journal of neuroscience : the official journal of the Society for Neuroscience 29 (13):4252-4262. doi:10.1523/JNEUROSCI.5572-08.2009

Mapes J, Chen YZ, Kim A, Mitani S, Kang BH, Xue D (2012) CED-1, CED-7, and TTR-52 Regulate Surface Phosphatidylserine Expression on Apoptotic and Phagocytic Cells. Current biology : CB 22 (14):1267-1275. doi:10.1016/j.cub.2012.05.052

Matozaki T, Murata Y, Okazawa H, Ohnishi H (2009) Functions and molecular mechanisms of the CD47-SIRPalpha signalling pathway. Trends Cell Biol 19 (2):72-80. doi:S0962-8924(08)00286-9 [pii]

10.1016/j.tcb.2008.12.001

Mizwicki MT, Menegaz D, Zhang J, Barrientos-Duran A, Tse S, Cashman JR, Griffin PR, Fiala M (2012) Genomic and nongenomic signaling induced by 1alpha,25(OH)2-vitamin D3 promotes the recovery of amyloid-beta phagocytosis by Alzheimer's disease macrophages. Journal of Alzheimer's disease : JAD 29 (1):51-62. doi:10.3233/JAD-2012-110560

Nguyen JV, Soto I, Kim KY, Bushong EA, Oglesby E, Valiente-Soriano FJ, Yang Z, Davis CH, Bedont JL, Son JL, Wei JO, Buchman VL, Zack DJ, Vidal-Sanz M, Ellisman MH, Marsh-Armstrong N (2011) Myelination transition zone astrocytes are constitutively phagocytic and have synuclein dependent reactivity in glaucoma. Proceedings of the National Academy of Sciences of the United States of America 108 (3):1176-1181. doi:10.1073/pnas.1013965108

Noda M, Suzumura A (2012) Sweepers in the CNS: Microglial Migration and Phagocytosis in the Alzheimer Disease Pathogenesis. International journal of Alzheimer's disease 2012:891087. doi:10.1155/2012/891087

Pihlaja R, Koistinaho J, Malm T, Sikkila H, Vainio S, Koistinaho M (2008) Transplanted astrocytes internalize deposited beta-amyloid peptides in a transgenic mouse model of Alzheimer's disease. Glia 56 (2):154-163. doi:10.1002/glia.20599

Seidel K, Vinet J, Dunnen WF, Brunt ER, Meister M, Boncoraglio A, Zijlstra MP, Boddeke HW, Rub U, Kampinga HH, Carra S (2012) The HSPB8-BAG3 chaperone complex is upregulated in astrocytes in the human brain affected by protein aggregation diseases. Neuropathology and applied neurobiology 38 (1):39-53. doi:10.1111/j.1365-2990.2011.01198.x

Shaftel SS, Kyrkanides S, Olschowka JA, Miller JN, Johnson RE, O'Banion M K (2007) Sustained hippocampal IL-1beta overexpression mediates chronic neuroinflammation and ameliorates Alzheimer plaque pathology. J Clin Invest 117 (6):1595-1604

Sick E, Boukhari A, Deramaudt T, Ronde P, Bucher B, Andre P, Gies JP, Takeda K (2011) Activation of CD47 receptors causes proliferation of human astrocytoma but not normal astrocytes via an Akt-dependent pathway. Glia 59 (2):308-319. doi:10.1002/glia.21102

Simard AR, Soulet D, Gowing G, Julien JP, Rivest S (2006) Bone marrow-derived microglia play a critical role in restricting senile plaque formation in Alzheimer's disease. Neuron 49 (4):489-502

Streit WJ, Braak H, Xue QS, Bechmann I (2009) Dystrophic (senescent) rather than activated microglial cells are associated with tau pathology and likely precede neurodegeneration in Alzheimer's disease. Acta Neuropathol 118 (4):475-485. doi:10.1007/s00401-009-0556-6

Van Amersfoort ES, Van Strijp JA (1994) Evaluation of a flow cytometric fluorescence quenching assay of phagocytosis of sensitized sheep erythrocytes by polymorphonuclear leukocytes. Cytometry 17 (4):294-301. doi:10.1002/cyto.990170404

Veerhuis R, Boshuizen RS, Morbin M, Mazzoleni G, Hoozemans JJ, Langedijk JP, Tagliavini F, Langeveld JP, Eikelenboom P (2005) Activation of human microglia by fibrillar prion protein-related peptides is enhanced by amyloid-associated factors SAP and C1q. Neurobiol Dis 19 (1-2):273-282. doi:S0969-9961(05)00009-4 [pii]

10.1016/j.nbd.2005.01.005

Wilkinson K, El Khoury J (2012) Microglial scavenger receptors and their roles in the pathogenesis of Alzheimer's disease. International journal of Alzheimer's disease 2012:489456. doi:10.1155/2012/489456

Wyss-Coray T, Loike JD, Brionne TC, Lu E, Anankov R, Yan F, Silverstein SC, Husemann J (2003) Adult mouse astrocytes degrade amyloid-beta in vitro and in situ. Nat Med 9 (4):453-457. doi:10.1038/nm838

nm838 [pii]

Zotova E, Holmes C, Johnston D, Neal JW, Nicoll JA, Boche D (2011) Microglial alterations in human Alzheimer's disease following Abeta42 immunization. Neuropathology and applied neurobiology 37 (5):513-524. doi:10.1111/j.1365-2990.2010.01156.x

FIGURE LEGENDS

Figure 1. Astrocytes, in a mixed glial culture, are phagocytic.

Mixed glial cells were incubated with fluorescently-labelled latex beads (green) for 2 h and stained with anti-GFAP (red; A). The fluorescent micrograph demonstrates cellular localisation of the latex beads. The arrow denotes a probable microglial cell due to its lack of positive GFAP staining. (B, C) Orthogonal projections of confocal z-stacks confirm intracellular localisation of

fluorescently-labelled latex beads (green) in a CD11b$^+$ microglial cell (red; B) and a GFAP$^+$ astrocyte (red; C). Lysotracker$^®$ was used to visualise lysosomes (red) within GFAP$^+$ astrocytes (green; D). Nuclei were counterstained using DAPI (blue). Scale bars at 20µM.

Figure 2. Cytochalasin D inhibited the uptake of fluorescently-labelled latex beads.

Mixed glia were pre-treated with cytochalasin D (1, 3 or 10µM) for 2 h and incubated with latex beads for a further 2 h. Uptake of latex beads by CD11b$^+$ (A) and CD11b$^-$ (B) cells was significantly decreased following pre-treatment with cytochalasin D (***p<0.001; ANOVA). Data are expressed as means + SEM (n=4). (C,D) Mixed glia were treated with cytochalasin D (1, 3 or 10µM) for 4 h and alamar blue (A) and LDH (B) assays were carried out. The data show that cytochalasin D had no effect on cell viability. Staurosporine (5µM) was used as a positive control and significantly reduced cell viability (C) and increased LDH activity (D; ***p<0.001; ANOVA). Data are expressed as means + SEM (n=3).

Figure 3. FITC-labelled Aβ uptake by CD11b$^+$ and CD11b$^-$ cells is concentration-dependent and inhibited by cytochalasin D.

Mixed glial cells were incubated with FITC-labelled Aβ (0.15, 0.45, 1.35, 3 or 10µM) for 2 h. Uptake of Aβ by CD11b$^+$ (A) and CD11b$^-$ (B) cells increased in a concentration-dependent manner (**p<0.01; ***p<0.001; ANOVA). Data are expressed as means + SEM (n=4). Representative FACS-plots for each concentration are presented (C). Pretreatment of cells with cytochalasin D (1, 3 or 10µM) for 2 h prior to incubation with FITC-labelled Aβ decreased uptake by CD11b$^+$ (D) and CD11b$^-$ (E) cells (**p<0.01; ***p<0.001; ANOVA), with significantly greater inhibition when cells were incubated with10µM, compared with 1 and 3µM, cytochalasin D ($^+$p<0.05; ANOVA). Data are expressed as means + SEM (n=4).

Figure 4. Intracellular localisation of FITC-labelled Aβ in microglia and astrocytes

Representative micrograph of a phagocytosing CD11b$^+$ microglial cell (red; A) and GFAP$^+$ astrocyte (red; B) in orthogonal projections of confocal z-stacks. After a 2 h incubation period, FITC-labelled Aβ (green) was internalized by CD11b$^+$ microglia and GFAP$^+$ astrocytes. Nuclei were counterstained using DAPI (blue).

Figure 5. Phagocytosis is associated with release of ROS.

Isolated primary astrocytes, microglia and rat peripheral blood mononuclear cells (PBMC) were incubated with opsonized-zymosan and luminol for 44 min while chemiluminescence was assessed at 2 minute intervals. Chemiluminescence readings were similar in microglia and astrocytes but significantly greater in PBMC ($p < 0.001$; ANOVA). All cell types mounted a significant phagocytic response compared with control ($p < 0.01$; ANOVA). Data are expressed as means + SEM (n=5).

Figure 6. Aβ increased phagocytosis of latex beads in microglia and astrocytes.

Isolated microglia or astrocytes were incubated with Aβ$_{1-40}$ (4.2μM) + Aβ$_{1-42}$ (5.8μM) or reverse peptide Aβ$_{40-1}$ (10μM) for 24 h *in vitro*. Aβ significantly increased mRNA expression of CD11b (A) and phagocytosis of latex beads by CD11b$^+$ cells (B, C; ***$p < 0.001$; *$p < 0.05$; Student's *t*-test for independent means). Aβ had no effect on mRNA expression of GLAST (D) but significantly increased expression of GLT-1 (E) and phagocytosis of latex beads by GLAST$^+$ cells (F,G; ***$p < 0.001$; Student's *t*-test for independent means). Data are expressed as means + SEM (n=4-6).

Figure 7. Aβ-induced phagocytosis of latex beads by astrocytes is attenuated by antibodies to Aβ binding proteins
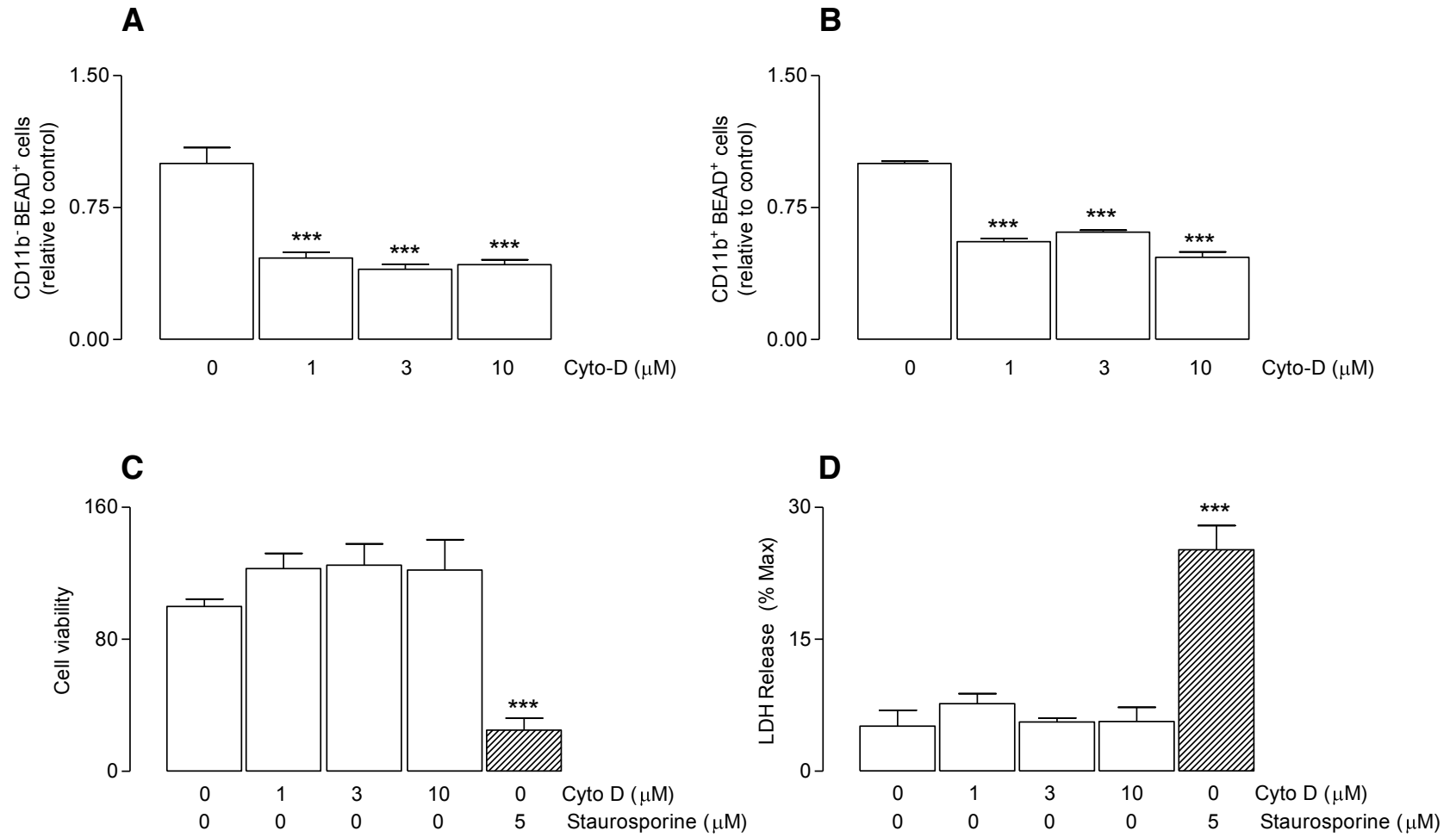
Aβ significantly increased expression of CD36 mRNA (A; ***$p < 0.001$; Student's *t*-test for independent means) and CD47 mRNA (C; **$p < 0.01$; Student's *t*-test for independent means)
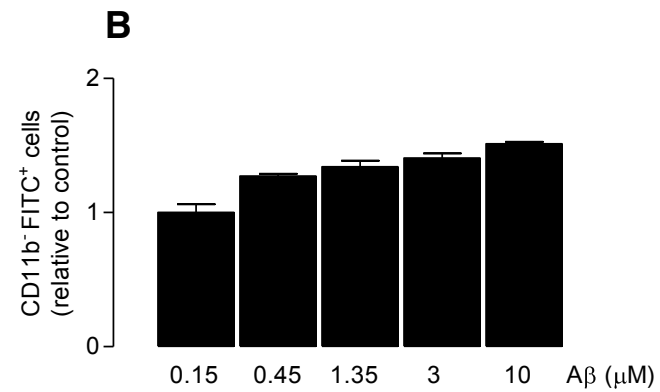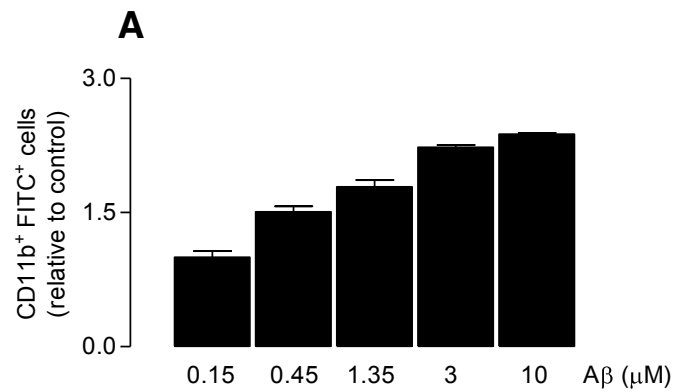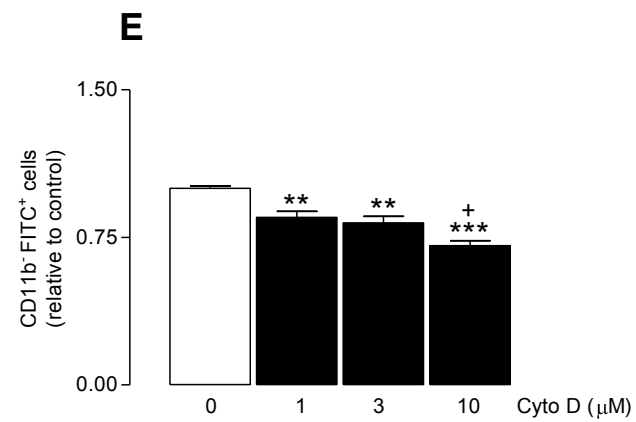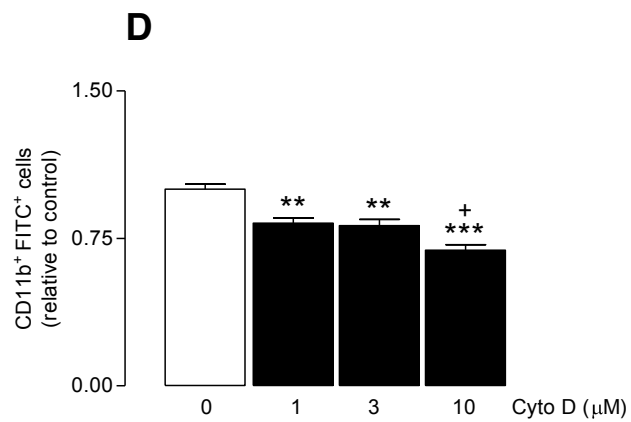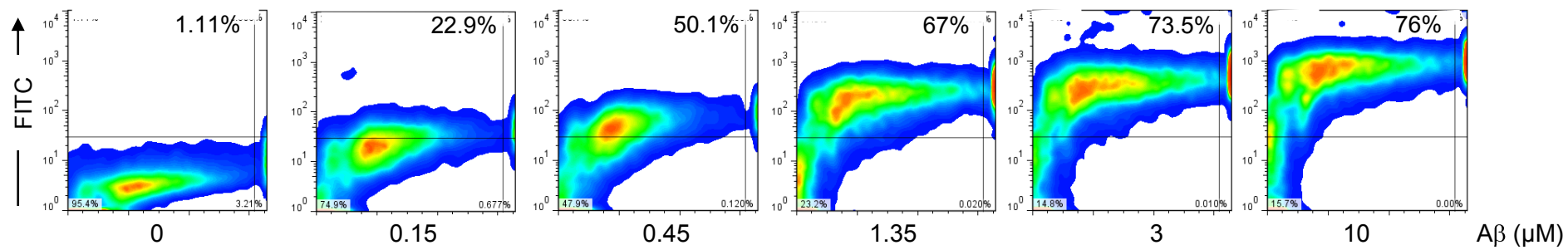
but significantly decreased RAGE mRNA (E; *p<0.05; Student's *t*-test for independent means). Aβ significantly increased uptake of latex beads by astrocytes (*p < 0.05; B,D,F); this effect was inhibited by incubation of cells in the presence of anti-CD36 (B), anti-CD47 (D) or anti-RAGE (F; $^+$p < 0.05; $^{++}$p < 0.01; ANOVA; Aβ in the presence of IgG vs Aβ in the presence of anti-CD36 or anti-CD47 or anti-RAGE). The antibodies also decreased unstimulated uptake of latex beads ($^+$p < 0.05; $^{++}$p < 0.01; ANOVA; control in the presence of IgG vs anti-CD36 or anti-CD47 or anti-RAGE; ANOVA).
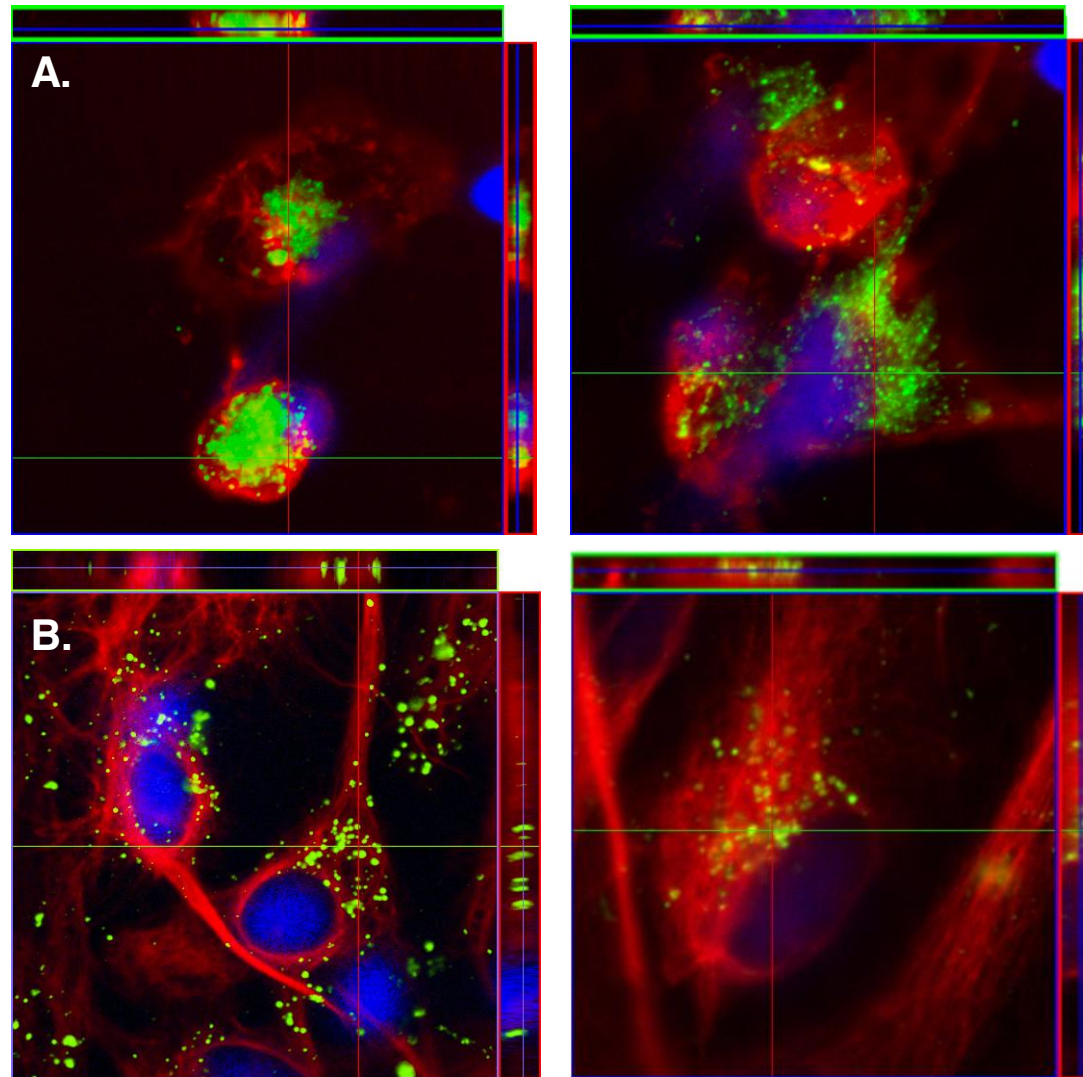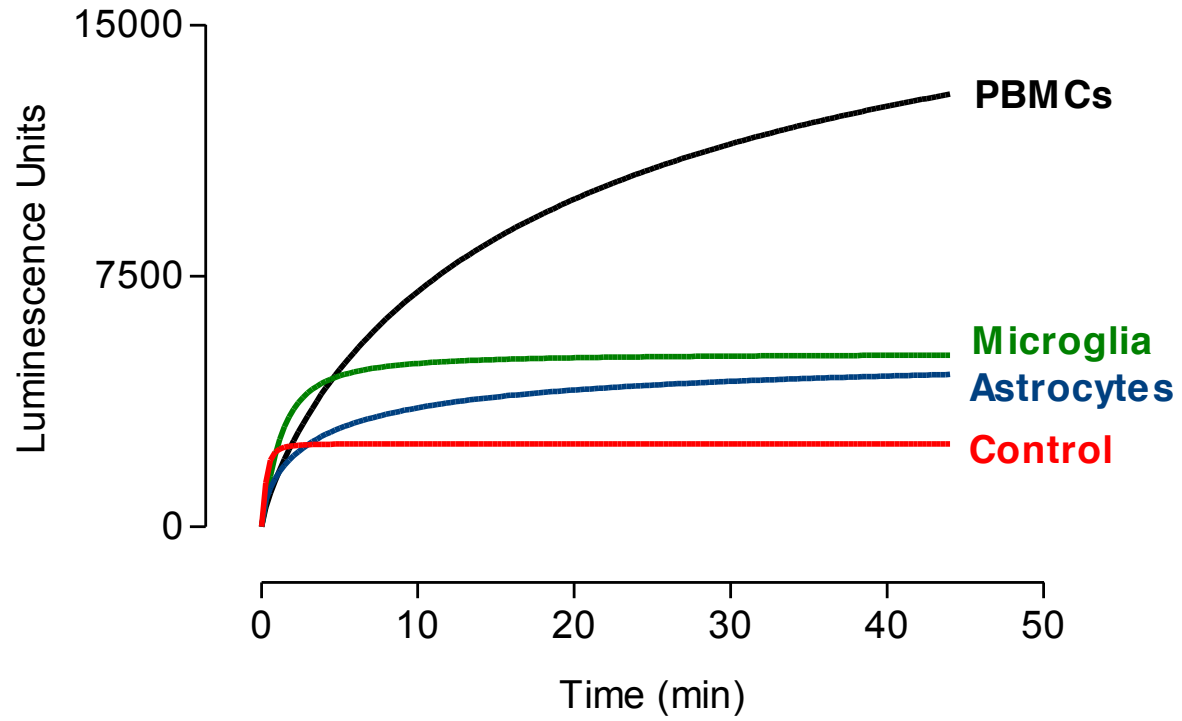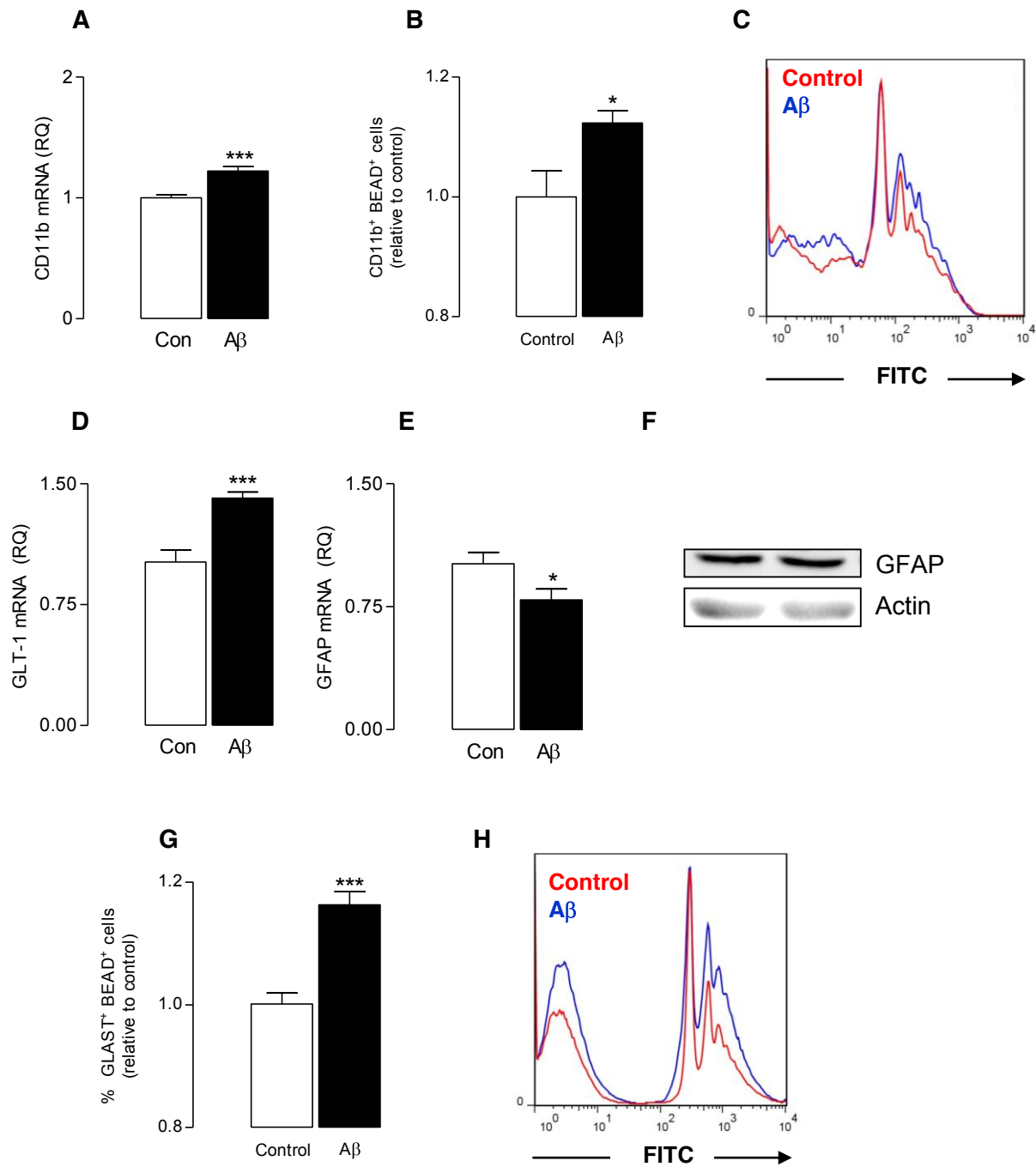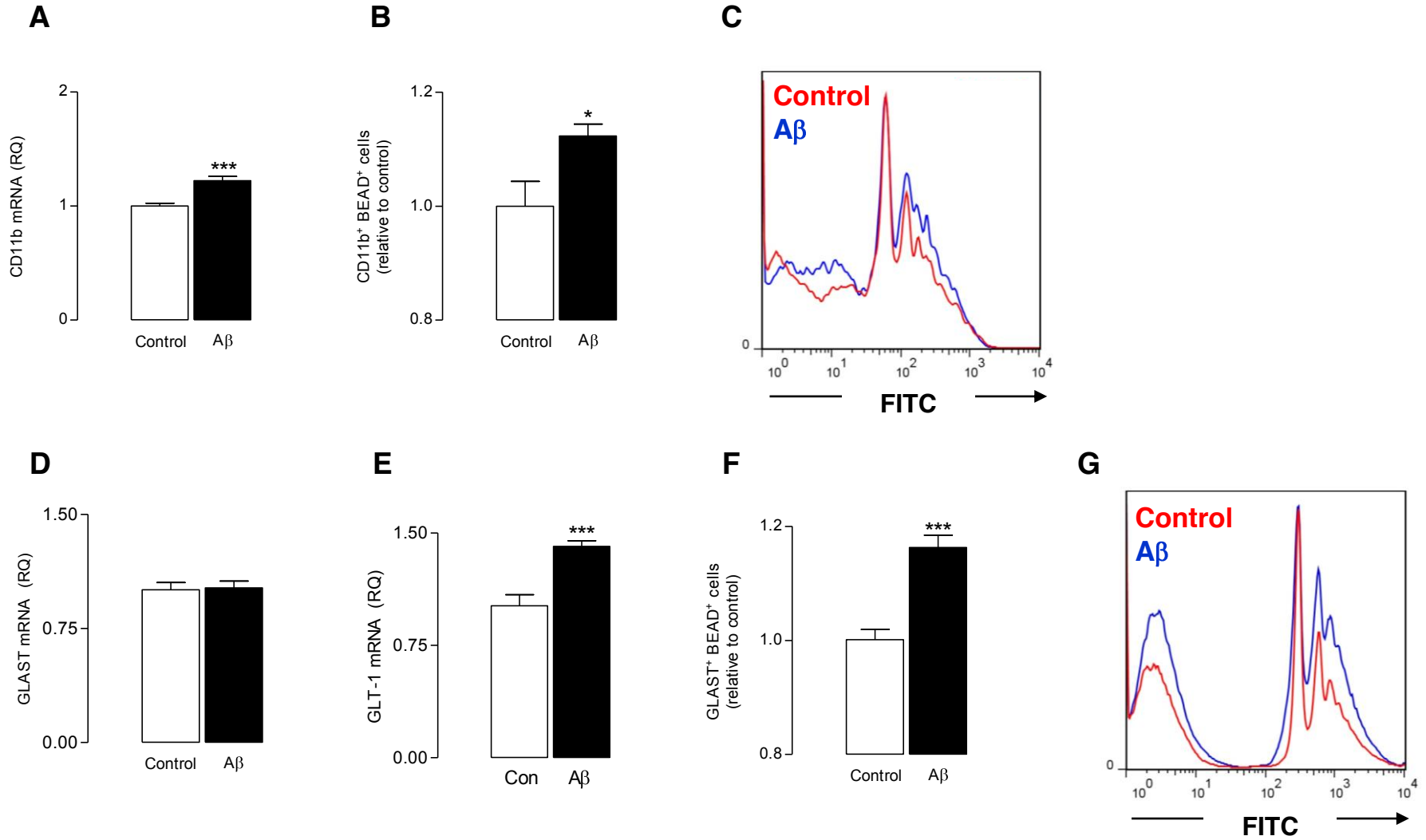
FIGURE 1
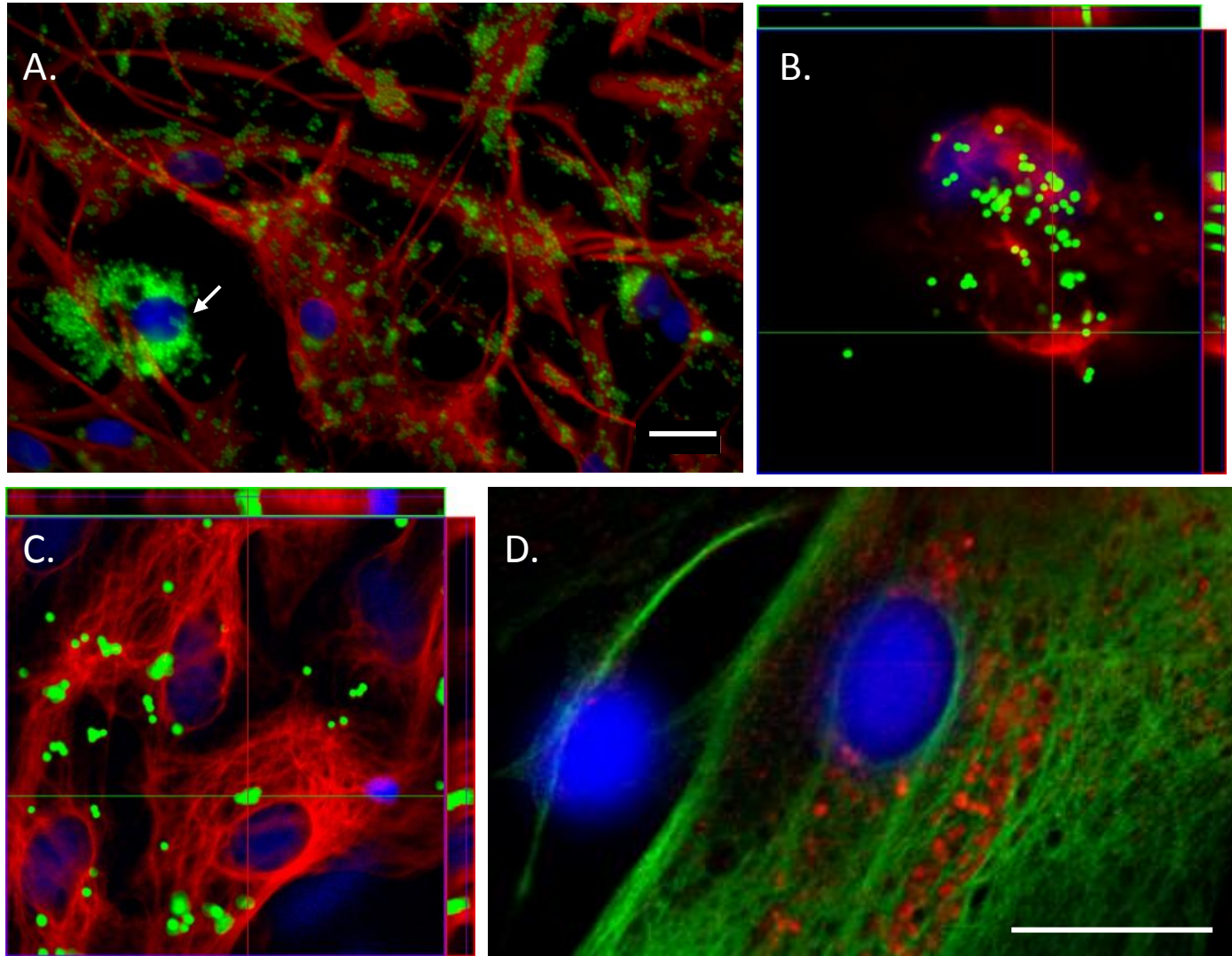
FIGURE 2

FIGURE 3

FIGURE 4

FIGURE 5

FIGURE 6

A

CD11b mRNA (RQ)

2 —
1 — ***
0 —
Control   Aβ

B

CD11b⁺ BEAD⁺ cells (relative to control)

1.2 — *
1.0 —
0.8 —
Control   Aβ

C

Control
Aβ

FITC

D

GLAST mRNA (RQ)

1.50 —
0.75 —
0.00 —
Control   Aβ

E

GLT-1 mRNA (RQ)

1.50 — ***
0.75 —
0.00 —
Con   Aβ

F

GLAST⁺ BEAD⁺ cells (relative to control)

1.2 — ***
1.0 —
0.8 —
Control   Aβ

G

Control
Aβ

FITC

FIGURE 7